Gradient algorithms for polygonal approximation of convex contours

Sara Susca [a], Francesco Bullo [a], Sonia Martínez [b]

[a] *Center for Control, Dynamical Systems and Computation, University of California at Santa Barbara, Santa Barbara, CA, 93106-5070, USA. Tel: (+1) 805 893-5169, Fax: (+1) 805 893-8651*

[b] *Mechanical and Aerospace Engineering Department, University of California at San Diego, 9500 Gilman Dr, La Jolla, CA, 92093-0411, USA. Tel: (+1) 858 822-4243, Fax: (+1) 858 534-4387*

Abstract

The subjects of this paper are descent algorithms to optimally approximate a strictly convex contour with a polygon. This classic geometric problem is relevant in interpolation theory and data compression, and has potential applications in robotic sensor networks. We design gradient descent laws for intuitive performance metrics such as the area of the inner, outer, and "outer minus inner" approximating polygons. The algorithms position the polygon vertices based on simple feedback ideas and on limited nearest-neighbor interaction.

Key words: convex body approximation, gradient methods, interpolation, motion coordination.

1 Introduction

In this paper we investigate algorithms to compute an approximating polygon for strictly convex planar contours. We require that the approximating polygon minimizes a certain meaningful error metric. In applications such as monitoring of environmental processes it is important to be able to approximate the contour of the region of interest. Finding efficient or optimal approximating polygons is also relevant in other applications like solving interpolation problems or data compression. Constructing an optimal polygonal approximation of a contour has been a research subject for mathematicians and engineers across the last three centuries. Still interesting problems continue to remain unsolved especially for the general setting of non-convex bodies. Boundary estimation and tracking is also a relevant problem in computer vision [7]. Some references on the boundary estimation problem for robotic sensor networks include [10,3,2,14]. A final motivation for this work is the interest in dynamical systems that solve optimization problems, as described for example in [5]; discrete-time gradient systems and discrete-time balancing algorithms for networks of agents are discussed in [1] and in [11].

Email addresses: sara@ece.ucsb.edu (Sara Susca), bullo@engineering.ucsb.edu (Francesco Bullo), soniamd@ucsd.edu (Sonia Martínez).

As pointed out by the authors in [6], in the XIX century it was known how to geometrically characterize the polygon enclosed in a convex body that minimizes the area difference between itself and the enclosing convex body. On the other hand, the geometric characterization of a polygon, enclosing a given strictly convex body, that again minimizes the difference of the areas is more complex and less intuitive. To the best of our knowledge, the earliest reference on this matter appeared only in 1949 by E. Trost, see [13]. In the XX century it was also proved that for a convex planar body the approximation error, for various useful metrics, goes to zero as $1/N^2$, where N is the number of vertices of the interpolating polygon. For a detailed list of references we refer to the survey [4].

Given N points (ordered in a counter-clockwise fashion) on a strictly convex contour, it is natural to define an enclosed (i.e., inscribed) polygon and an enclosing (i.e., circumscribed) polygon to the contour. Here the faces of the enclosing polygon are subsets of the tangent lines to the strictly convex contour. We adopt three geometrically-motivated error metrics that the approximating polygon can minimize. They are described as follows. The first two metrics we consider are the difference between the area enclosed in the contour and the following areas: the inner polygon area and the outer polygon area. The third metric is the difference between the area of the outer polygon and the area of the inner polygon. We derive the expressions, two of which are novel contributions of this paper, of the error metrics as functions of the vertex positions of the approximating polygon. We propose three gradient descent vector fields for N points to dynamically construct the optimal approximating polygon. The vector fields rely only on local information about the contour and about the immediate clockwise and counter-clockwise neighboring vertices. This property allows the vector fields to be implemented by a network of robots. The robots, placed around the boundary of a convex set, have to be able to sense the tangent of the set, to communicate with each other, and to move. We analyze the dynamical system behavior of these vector fields and present simulation results. We also present discrete-time versions that allows the nodes to reach locally optimal configurations for two of the metrics introduced.

The paper is organized as follows. In Section 2 we define some notation and the three performance metrics. In Sections 3 and 4 we present the continuous time gradient descent algorithms and their respective discrete time versions to compute the best inner and outer approximating polygon, while in Section 5 we present an algorithm to construct the polygon minimizing the "outer minus inner" area. In Section 6 we present some simulation results.

2 Problem setup

Let $\bar{\mathbb{R}} = \mathbb{R} \cup \{+\infty, -\infty\}$. Let $Q \subseteq \mathbb{R}^2$ be a bounded, strictly convex body with a twice differentiable boundary ∂Q. Let $\mathbb{T} \subseteq \mathbb{R}^2$ denote the unit circle. We parameterize ∂Q by a map $\gamma\colon \mathbb{T} \to \partial Q$, and represent its signed curvature by $\kappa\colon \mathbb{T} \to \mathbb{R}$. Note that κ remains positive as we traverse the curve γ in a counter-clockwise manner. For $s_i \in \mathbb{T}, i \in \{1, \dots, N\}$, let $p_i = \gamma(s_i) = (x_i, y_i) \in \partial Q$ be the position of N points on the boundary ordered in counter-clockwise direction. We assume $N \geq 3$ and use the identification $0 \equiv N$ and $N + 1 \equiv 1$. For $s \in \mathbb{T}$, let $\mathbf{t}(s)$ and $\mathbf{n}(s)$ denote the tangent vector $\gamma'(s)$ and the unit outward normal vector at $\gamma(s) \in \partial Q$. With a slight abuse of notation, we sometimes refer to unit tangent and normal vectors at the point p_i as $\mathbf{t}_i$ and $\mathbf{n}_i$, and at the point $p \in \partial Q$ as $\mathbf{t}(p)$ and $\mathbf{n}(p)$. For $p \in \partial Q$, define the half-plane $\mathcal{H}(p) = \{z \in \mathbb{R}^2 \mid (p - z) \cdot \mathbf{n}(p) \leq 0\}$; see Figure 1. Given two points A and B, let $\overline{AB}$ denote the segment between them.

Definition 2.1 (Inner and outer polygons) *Let $p_1, \dots, p_N$ be the positions of N points on ∂Q and let $\mathcal{P}(\mathbb{R}^2)$ denote the parts of $\mathbb{R}^2$. Let us define $P_I\colon (\partial Q)^N \to \mathcal{P}(\mathbb{R}^2)$ by $P_I(p_1, \dots, p_n) = \mathrm{co}(p_1, \dots, p_n)$, the* inner polygon *generated by the vertices $\{p_1, \dots, p_n\}$. With a slight abuse of notation, let us define the* possibly unbounded outer polygon *$P_O\colon (\partial Q)^N \to \mathcal{P}(\mathbb{R}^2)$ by $P_O(p_1, \dots, p_N) = \mathcal{H}(p_1) \cap \dots \cap \mathcal{H}(p_N)$.*

Definition 2.2 (Tangent lines and tangent connections) *Define the rays $\ell^+\colon \partial Q \to \mathcal{P}(\mathbb{R}^2)$ and $\ell^-\colon \partial Q \to \mathcal{P}(\mathbb{R}^2)$ by $\ell^+(p) = \{p + \lambda \mathbf{t}(p) \mid \lambda \geq 0\}$ and $\ell^-(p) = \{p + \lambda \mathbf{t}(p) \mid \lambda \leq 0\}$, respectively. Also, let $\ell(p) = \ell^+(p) \cup \ell^-(p)$. A pair (p, q) of points in ∂Q is* counter-clockwise tangent-connected *(abbreviated cc-tangent-connected) if $\ell^+(p) \cap \ell^-(q) \neq \emptyset$.*

The following result is illustrated in Figure 1.

Lemma 2.3 (Bounded outer polygon) *All pairs (p_i, p_{i+1}), $i \in \{1, \dots, N\}$, are cc-tangent-connected if and only if $P_O(p_1 \dots, p_N)$ is bounded.*

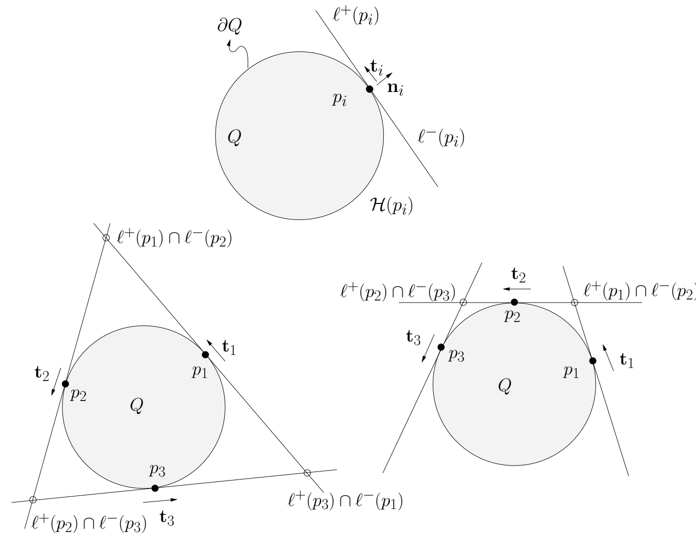

Fig. 1. From left to right: the half-plane $\mathcal{H}(p_i)$ and its boundary $\ell(p_i) = \ell^+(p_i) \cup \ell^-(p_i)$, three points defining a bounded outer polygon, and three points defining an unbounded outer polygon.

Definition 2.4 (Error metrics) *We quantify the approximation error of Q through three different metrics:*

- *The* inner set approximation error *$E_I\colon (\partial Q)^N \to \mathbb{R}_+$ is defined by $E_I(p_1, \dots, p_n) = \mathrm{Area}(Q \backslash P_I(p_1, \dots, p_n))$.*
- *The* outer set approximating error *$E_O\colon (\partial Q)^N \to \bar{\mathbb{R}}_+$ is defined by $E_O(p_1, \dots, p_n) = \mathrm{Area}(P_O(p_1, \dots, p_n) \setminus Q)$.*
- *The* symmetric difference error *$E_S\colon (\partial Q)^N \to \bar{\mathbb{R}}_+$ is defined by $E_S(p_1, \dots, p_n) = \mathrm{Area}(P_O(p_1, \dots, p_n) \setminus P_I(p_1, \dots, p_n))$.*

Remark 2.5 (Implementation by group of robots) In what follows we present descent algorithms for the minimization of these error metrics. The algorithms can be implemented by group of robots where we regard p_i as a robot that can sense a portion of ∂Q, communicate with some robots and move to improve the approximation of ∂Q. For all the algorithms that follow we establish how much sensing and communication are required. •

3 Inner-polygon approximation algorithms

The algorithms of this section are based on the interpolation error E_I. Observe that $E_I(p_1,\dots,p_N) = \text{Area}(Q) - \text{Area}(P_I(p_1,\dots,p_N))$. Recalling that the set of points $\{p_1,\dots,p_N\}$ is ordered in counter-clockwise direction, and that (x_i, y_i) are coordinates of p_i, then an expression for $\text{Area}(P_I(p_1,\dots,p_N))$ is:

$$\text{Area}(\mathcal{P}_I(p_1,\dots,p_N)) = \frac{1}{2}\sum_{i=1}^{N}(x_i y_{i+1} - x_{i+1} y_i)\,.$$

We now define a dynamical system by projecting the ith component of the gradient of E_I on the tangent $\mathbf{t}_i$:

$$\begin{aligned} \dot{p}_i &= \left(\mathbf{t}_i \cdot \frac{\partial\,\text{Area}(P_I(p_1,\dots,p_N))}{\partial p_i}\right)\mathbf{t}_i \qquad (1)\\ &= \left(\frac{1}{2}\mathbf{t}_i^T \begin{pmatrix} y_{i+1} - y_{i-1} \\ x_{i-1} - x_{i+1}\end{pmatrix}\right)\mathbf{t}_i\,, \quad i \in \{1,\dots,N\}\,. \end{aligned}$$

Lemma 3.1 (Gradient flow for E_I) *If $t \mapsto \eta(t) = (p_1(t),\dots,p_N(t))$ denotes a trajectory of the dynamical system (1), then $E_I \circ \eta$ is monotonic non-increasing and η converges asymptotically to the set of critical configurations of E_I. A configuration $p_1,\dots,p_N$ is critical for E_I if and only if, for all $i \in \{1,\dots,N\}$,*

$$\mathbf{t}_i \perp \begin{pmatrix} y_{i+1} - y_{i-1} \\ x_{i-1} - x_{i+1}\end{pmatrix}, \qquad (2)$$

that is, $\mathbf{n}_i \perp (p_{i+1} - p_{i-1})$. Furthermore, if the boundary ∂Q is analytic, then η converges asymptotically to a critical configuration.

PROOF. It is easy to see that $\dot{p}_i(t) = -\frac{\partial E_I(t)}{\partial p_i}|_{\partial Q}$ therefore (1) is a gradient system. As a consequence, E_I is monotonic non-increasing:

$$\begin{aligned} \frac{dE_I}{dt} &= -\frac{\text{Area}(\mathcal{P}_I(p_1,\dots,p_N))}{dt}\\ &= -\sum_{i=1}^{N}\left(\mathbf{t}_i \cdot \frac{\partial\,\text{Area}(P_I(p_1,\dots,p_N))}{\partial p_i}\right)^2 \mathbf{t}_i \le 0, \end{aligned}$$

and the p_i's asymptotically converge to the set of critical configurations of E_I. If the boundary ∂Q is analytic, then E_I is analytic (because it is a composition of analytic functions) and, by [9], we can conclude that every trajectory has finite length and tends to a single point belonging to the set of critical configurations.

Not every critical point of E_I is an extremum of E_I: Figure 2 illustrates a saddle point of E_I.

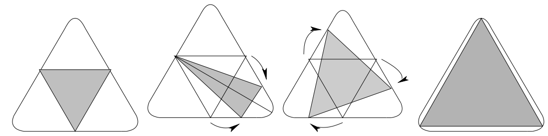

Fig. 2. From left to right: saddle point configuration, nearby configuration that increases the error E_I, bear by configuration that decreases the error E_I, configuration corresponding to a minimum error configuration.

Remark 3.2 (Historical notes) The characterization (2) of the critical configurations was already obtained in the XIX century according to [6]. The paper [6] additionally shows how the critical point configurations satisfy the condition that points remain closer in regions of higher mean curvature, which is a desirable condition for shape representation. It is believed [4] that as the number of nodes increases, the type of configurations that satisfy (2) correspond only to global error minima.•

Remark 3.3 (Implementation by group of robots) In the dynamical system (1), the velocity $\dot{p}_i$ depends only on p_{i-1}, p_{i+1}, and $\mathbf{t}_i$. Therefore, to implement this velocity control, every robot has to receive information about the positions of its immediate clockwise and counter-clockwise neighbors and sense the gradient of the contour at its position. Clearly, the communication graph is a ring graph. •

3.1 Discrete-time inner-polygon approximation algorithms

Here we present two discrete-time versions of the vector field in equation (1).

Given a strictly convex set Q, define $q_{\max}\colon (\partial Q)^2 \to \partial Q$ as follows: $q_{\max}(q_1, q_2)$ is the point of the counterclockwise arc from q_1 to q_2 whose tangent to ∂Q is parallel to the segment $\overline{q_1 q_2}$. Note that $q_{\max}(q_1, q_2)$ maximizes $q \mapsto \text{Area}(P_I(q_1, q, q_2))$.

Algorithm 1. At each discrete time instant $k \in \mathbb{N}$ and for each node $i \in \{1,\dots,N\}$ define:

$$p_i(k+1) = \begin{cases} q_{\max}(p_{i-1}(k), p_{i+1}(k)), & \text{if } i \equiv k \mod N,\\ p_i(k), & \text{if } i \not\equiv k \mod N\,. \end{cases} \qquad (3)$$

Proposition 3.4 (Convergence of Algorithm 1) *If $k \mapsto \eta(k) = (p_1(k),\dots,p_N(k))$ denotes a trajectory of the dynamical system (3), then $E_I \circ \eta$ is monotonic non-increasing and η converges asymptotically to the set of critical configurations of E_I.*

PROOF. Let $A_k = \text{Area}(P_I(p_1(k),\dots,p_N(k))$ and let i be congruent mod N with k. We have that $A_k =$

$T_k + \bar{A}_k$, where $T_k = \text{Area}(P_I(p_{i-1}(k), p_i(k), p_{i+1}(k))$ and $\bar{A}_k$ is the area of the inner polygon generated by the complementary set of nodes. Since $q_{\max}(q_1, q_2)$ maximizes $q \mapsto \text{Area}(P_I(q_1, q, q_2))$, $T_k = \text{Area}(P_I(p_{i-1}(k), p_i(k), p_{i+1}(k)) \leq \text{Area}(P_I(p_{i-1}(k), p_i(k+1), p_{i+1}(k)) = T_{k+1}$. Therefore, $A_k = T_k + \bar{A}_k \leq T_{k+1} + \bar{A}_k = A_{k+1}$, i.e., the point that moves at time k does so in order to increase the area of the inner polygon or, equivalently, to decrease the error E_I. Using the extension of the LaSalle Invariance Principle for discrete-time systems ([8]) we can claim that the p_i's will asymptotically reach the largest weakly invariant set in $\{(p_1(k), \dots, p_N(k)) \in \partial Q^N | E_I \circ \eta(k+1) - E_I \circ \eta(k) = 0\}$, which is the set of critical configurations for E_I.

The quintuplet $(p_{-2}, p_{-1}, p_0, p_1, p_2)$ is *admissible* if the following three inequalities hold:

$$\begin{aligned}
&\text{Area}(P_I(q_{\max}(p_{-2}, p_0), p_0, q_{\max}(p_0, p_2)))\\
&\quad \leq \text{Area}(P_I(q_{\max}(p_{-2}, p_0), q_{\max}(p_{-1}, p_1), q_{\max}(p_0, p_2))),\\
&\text{Area}(P_I(p_{-1}, p_0, q_{\max}(p_0, p_2)))\\
&\quad \leq \text{Area}(P_I(p_{-1}, q_{\max}(p_{-1}, p_1), q_{\max}(p_0, p_2))),\\
&\text{Area}(P_I(q_{\max}(p_{-2}, p_0), p_0, p_1))\\
&\quad \leq \text{Area}(P_I(q_{\max}(p_{-2}, p_0), q_{\max}(p_{-1}, p_1), p_1)).
\end{aligned}$$

Algorithm 2. At each discrete time instant $k \in \mathbb{N}$ and for each node $i \in \{1, \dots, N\}$ define:

$$p_i(k+1) = q_{\max}(p_{i-1}(k), p_{i+1}(k)), \qquad (4)$$

if $(p_{i-2}(k), p_{i-1}(k), p_i(k), p_{i+1}(k), p_{i+2}(k))$ is admissible, and $p_i(k+1) = p_i(k)$ otherwise. Here is our main analysis result in this section.

Proposition 3.5 (Convergence of Algorithm 2) *E_I is monotonic non-increasing along all trajectories of* (4).

PROOF. The proof consists of two parts. As first fact (i), we prove inductively that the area of any polygon of N vertices increases by leaving any two consecutive nodes fixed and by moving the other $N-2$ vertices according to (4). As second fact (ii), building on the previous result, we show that the area of any polygon of N vertices increases by moving the all the N vertices according to (4).

Let us prove first (i) by induction on the number of vertices of a polygon. Let us consider $N = 3$. Clearly, if two of the three vertices are fixed and the other one moves according to (4), the area of the triangle formed by the three nodes increases, just as seen for Algorithm 1. Assume now that, given a polygon $P_I(p_1, \dots, p_{N-1})$ with $N-1$ vertices, its area can be increased by leaving any two consecutive nodes fixed and moving the other $N-1-2$ vertices according to (4). Let us now prove that the same property holds for the polygon $P_I(p_1, \dots, p_N)$ with N vertices. Clearly, we have that:

$$\begin{aligned}
\text{Area}(P_I(p_1, \dots, p_N)) = {}& \text{Area}(P_I(p_1, \dots, p_{N-1}))\\
&+ \text{Area}(P_I(p_{N-1}, p_N, p_1)),
\end{aligned}$$

where for simplicity of notation we dropped the time index k. By assumption, the area of a polygon with $N-1$ vertices increases if any two consecutive points are fixed and the rest moves according to (4). Therefore, we have

$$\begin{aligned}
&\text{Area}(P_I(p_1, p_2 \dots, p_{N-2}, p_{N-1}))\\
&\qquad \leq \text{Area}(P_I(p_1, p_2^+ \dots, p_{N-2}^+, p_{N-1})),
\end{aligned}$$

where for simplicity of notation the superscript + indicates that the node has updated its position according to (4). This implies:

$$\begin{aligned}
&\text{Area}(P_I(p_1, \dots, p_N))\\
&\leq \text{Area}(P_I(p_1, p_2^+ \dots, p_{N-2}^+, p_{N-1})) + \text{Area}(P_I(p_{N-1}, p_N, p_1))\\
&= \text{Area}(P_I(p_2^+ \dots, p_{N-2}^+, p_{N-1}, p_N)) + \text{Area}(P_I(p_N, p_1, p_2^+))\\
&\leq \text{Area}(P_I(p_2^+ \dots, p_{N-2}^+, p_{N-1}, p_N)) + \text{Area}(P_I(p_N, p_1^+, p_2^+))\\
&= \text{Area}(P_I(p_1^+, p_2^+, \dots, p_{N-2}^+, p_{N-1}, p_N)).
\end{aligned}$$

The second inequality holds because along the trajectories of (4) we have that $\text{Area}(P_I(p_N, p_1, p_2^+)) \leq \text{Area}(P_I(p_N, p_1^+, p_2^+))$. This concludes the proof of (i). To prove (ii), note that

$$\begin{aligned}
&\text{Area}(P_I(p_1^+, p_2^+, \dots, p_{N-2}^+, p_{N-1}, p_N))\\
&= \text{Area}(P_I(p_1^+, \dots, p_{N-2}^+, p_{N-1})) + \text{Area}(P_I(p_{N-1}, p_N, p_1^+))\\
&\leq \text{Area}(P_I(p_1^+, \dots, p_{N-2}^+, p_{N-1})) + \text{Area}(P_I(p_{N-1}, p_N^+, p_1^+))\\
&= \text{Area}(P_I(p_N^+, p_1^+, \dots, p_{N-2}^+)) + \text{Area}(P_I(p_{N-2}^+, p_{N-1}, p_N^+))\\
&\leq \text{Area}(P_I(p_N^+, p_1^+, \dots, p_{N-2}^+)) + \text{Area}(P_I(p_{N-2}^+, p_{N-1}^+, p_N^+))\\
&= \text{Area}(P_I(p_1^+, \dots, p_N^+)).
\end{aligned}$$

Remark 3.6 Stationary configurations of (4) are not necessarily critical points of E_I, i.e., at an equilibrium configuration for (4) there could exist a node for which condition (2) is not satisfied. A set of nodes could be "unlocked" by running a leader-election algorithm between neighbors and giving priority of motion to the consensual leader. This operation respects the descent nature of the algorithm and guarantees that we reach a desired critical configuration. •

Remark 3.7 (Implementation by group of robots) To implement Algorithm 1, each robot p_i needs to have knowledge about its own label number $i \in \{1, \dots, N\}$ and about the position of its one-hop neighbors. Algorithm 2, does not require a labeling of robots, but requires each robot to have knowledge about part of the contour and knowledge about the position of its two-hop neighbors. •

4 Outer-polygon approximation algorithms

The algorithms of this section are based on the interpolation error E_O. We begin with a geometric characterization of the partial derivative of E_O and of the critical configurations for E_O. First, for $i \in \{1, \dots, N\}$, we define $\alpha_i(p_i, p_{i+1})$ to be the angle (measured in counter-clockwise order) from $\mathbf{t}_i$ to $\mathbf{t}_{i+1}$. Assuming any pair (p_i, p_{i+1}) is cc-tangent-connected, consider $A_i = \ell^-(p_i) \cap \ell^+(p_{i-1})$ and $B_i = \ell^-(p_{i+1}) \cap \ell^+(p_i)$. Let us denote by d_i^- (resp. d_i^+) the length of the segment $\overline{p_i A_i}$ (resp. the segment $\overline{p_i B_i}$), as in Figure 3(a). It is

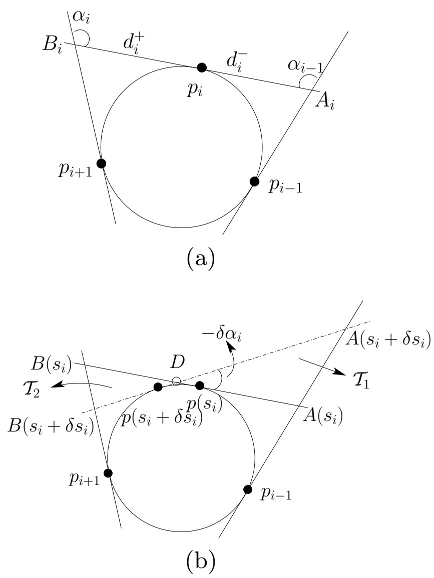

Fig. 3. (a) Illustration of α_i, α_{i-1}, A_i and B_i. (b) Variation of E_O described in Proposition 4.1.

useful to define $d_i^- = +\infty$ (resp. $d_i^+ = +\infty$) when the pair (p_{i-1}, p_{i+1}) is not cc-tangent-connected. One can show that:

$$d_i^-(p_i, p_{i-1}) = \begin{cases} +\infty\,, & \text{if } p_i \neq p_{i-1} \\ & \text{and } \mathbf{t}_i \cdot \mathbf{n}_{i-1} = 0, \\ \dfrac{(p_i - p_{i-1}) \cdot \mathbf{n}_{i-1}}{\mathbf{t}_i \cdot \mathbf{n}_{i-1}}\,, & \text{otherwise}\,, \end{cases}$$

$$d_i^+(p_i, p_{i+1}) = \begin{cases} +\infty\,, & \text{if } p_i \neq p_{i+1} \\ & \text{and } \mathbf{t}_i \cdot \mathbf{n}_{i+1} = 0\,, \\ \dfrac{(p_{i+1} - p_i) \cdot \mathbf{n}_{i+1}}{\mathbf{t}_i \cdot \mathbf{n}_{i+1}}\,, & \text{otherwise}\,. \end{cases}$$

Proposition 4.1 (Partial derivative of E_O) *If all the pairs (p_i, p_{i+1}) are cc-tangent-connected, then*

$$\frac{\partial E_O(p_1, \dots, p_n)}{\partial s_i} = \frac{1}{2}(d_i^- + d_i^+)(d_i^- - d_i^+)\kappa(s_i).$$

PROOF. Let us consider $p(s_i)$ and $p(s_i + \delta s_i)$, two points on the arc from p_{i-1} to p_{i+1}, as shown in Figure 3(b). Let $D = \ell^+(s_i) \cap \ell^-(s_i + \delta s_i)$. Let $\delta\alpha_i = \alpha(s_i + \delta_i) - \alpha(s_i)$. Note that $\delta\alpha_i < 0$ when $\delta s_i > 0$. By construction:

$$\begin{aligned}\text{Area}(\mathcal{T}_1) - \text{Area}(\mathcal{T}_2) = E_O(&p_1, \dots, p(s_i + \delta s_i), \dots p_n) \\ &- E_O(p_1, \dots, p(s_i), \dots, p_n),\end{aligned}$$

where $\mathcal{T}_1$ is the triangle with vertices D, $A(s_i)$, and $A(s_i + \delta s_i)$, and $\mathcal{T}_2$ is the triangle with vertices D, $B(s_i)$, and $B(s_i + \delta s_i)$. We now prove that $\text{Area}(\mathcal{T}_1) = (d_i^-)^2(-\delta\alpha_i) + o(\delta\alpha_i^2)$ and that $\text{Area}(\mathcal{T}_2) = (d_i^+)^2(-\delta\alpha_i) + o(\delta\alpha_i^2)$, for small δs_i. Note that $\|p(s_i + \delta s_i) - p(s_i)\| = \|\gamma'(s_i)\delta s_i\| + o(\delta s_i^2)$ and that $\frac{\partial\alpha(s)}{\partial s} = \frac{\partial\alpha(s)}{\partial\mathbf{t}(s)}\frac{\partial\mathbf{t}(s)}{\partial s} = -\kappa(s)$. Therefore, we have $\delta\alpha_i = -\kappa(s_i)\delta s_i + o(\delta s_i^2)$. In fact, provided that $p_i \neq p_{i+1}$, the function $\alpha_i(p_i, p_{i+1})$ is differentiable and its gradient is: $\frac{\partial\alpha_i(p_i,p_{i+1})}{\partial\mathbf{t}_i} = (t_i^2, -t_i^1)$, where $\mathbf{t}_i = (t_i^1, t_i^2)$. Clearly, $\dfrac{\partial\mathbf{t}_i}{\partial s_i} = (-t_i^2, t_i^1)\kappa(s_i)$. It can be shown that $\|D - A(s_i)\| = d_i^- + \frac{\|\gamma'(s_i)\delta s_i\|}{2} + o(\delta s_i^2)$. Let h be the height of the triangle $\mathcal{T}_1$ with respect to the base $\|D - A(s_i)\|$. Clearly, we have $h = \|A(s_i) - A(s_i + \delta s_i)\| \sin(\alpha_{i-1})$ and

$$\frac{\|A(s_i) - A(s_i + \delta s_i)\|}{\sin(-\delta\alpha_i)} = \frac{\|D - A(s_i)\|}{\sin(\pi - (\alpha_{i-1} - \delta\alpha_i))},$$

and, therefore,

$$h = \|D - A(s_i)\| \frac{\sin(-\delta\alpha_i)}{\sin(\alpha_{i-1} - \delta\alpha_i)} \sin(\alpha_{i-1}).$$

We have then:

$$\begin{aligned}\text{Area}(\mathcal{T}_1) &= \frac{1}{2}\|D - A(s_i)\| h \\ &= \frac{1}{2}\|D - A(s_i)\|^2 \frac{\sin(\alpha_{i-1})}{\sin(\alpha_{i-1} - \delta\alpha_i)} \sin(-\delta\alpha_i).\end{aligned}$$

For small δs_i, and hence small $\delta\alpha_i$, we have that $\frac{\sin(\alpha_{i-1})}{\sin(\alpha_{i-1} - \delta\alpha_i)} = 1 + o(\delta\alpha_i)$, and $\sin(-\delta\alpha_i) = -\delta\alpha_i + o(\delta\alpha_i^2)$. Therefore:

$$\text{Area}(\mathcal{T}_1) = \frac{1}{2}(d_i^-)^2(-\delta\alpha_i) + o(\delta\alpha_i^2).$$

Analogously, it can be proved that $\text{Area}(\mathcal{T}_2) = \frac{1}{2}(d_i^+)^2(-\delta\alpha_i) + o(\delta\alpha_i^2)$. We can now compute

$$\begin{aligned}\frac{\partial E_O(p_1,\dots,p_n)}{\partial s_i} &= \lim_{\delta s_i\to 0}\frac{\text{Area}(\mathcal{T}_1)-\text{Area}(\mathcal{T}_2)}{\delta s_i},\\ &= \lim_{\delta s_i\to 0}\frac{1}{2}((d_i^+)^2-(d_i^-)^2)\frac{\delta\alpha_i}{\delta s_i},\\ &= \frac{1}{2}(d_i^- + d_i^+)(d_i^- - d_i^+)\kappa(s_i).\end{aligned}$$

where we used the fact that $\partial\alpha_i/\partial s_i = \kappa$.

Based on these notions and concepts, we define the dynamical system

$$\dot{p}_i = \text{sat}_v((d_i^+)^2 - (d_i^-)^2)\,\mathbf{t}_i\,, \qquad i\in\{1,\dots,N\}, \quad (5)$$

where the function $\text{sat}_v\colon \overline{\mathbb{R}}\to\mathbb{R}$, defined for some positive saturation value $v\in(0,+\infty)$, is given by:

$$\text{sat}_v(x) = \begin{cases} x\,, & |x|\le v,\\ \frac{x}{|x|}\,v\,, & |x|\ge v\,. \end{cases}$$

Equation (5) is well defined if we adopt the convention $|\pm\infty| = +\infty$, and the usual operations in $\overline{\mathbb{R}}$. We are ready for the main result of this section; note that the characterization of the critical points of E_O was originally given in [13].

Proposition 4.2 (Gradient flow for E_O) *If $t\mapsto\eta(t) = (p_1(t),\dots,p_N(t))$ denotes a trajectory of the dynamical system* (5)*, then (i) $E_O\circ\eta$ is bounded in finite time and monotonic non-increasing afterwards, and (ii) η converges asymptotically to the set of critical configurations of E_O. A configuration $p_1,\dots,p_N$ is critical for E_O if and only if, for all $i\in\{1,\dots,N\}$,*

$$d_i^+(p_i,p_{i+1}) = d_i^-(p_i,p_{i-1}).$$

Furthermore, if the boundary ∂Q is analytic, then η converges asymptotically to a critical configuration.

PROOF. Suppose that there exists $i\in\{1,\dots,N\}$ such that (p_i,p_{i+1}) is not cc-tangent-connected (i.e., $d_i^- < +\infty$ and $d_i^+ = +\infty$). Since $d_i^+ = +\infty$ also $d_{i+1}^- = +\infty$ and E_O is unbounded. Since ∂Q is strictly convex, we have $d_j^- < +\infty$ (resp. $d_j^+ < +\infty$), for all $j\notin\{i,i+1\}$. Because of equation (5), p_i will move counter-clockwise with speed $v>0$, while p_{i+1} will move clockwise with the same speed. Therefore, in finite time the two rays ℓ_i^+ and ℓ_{i+1}^- intersect, (p_i,p_{i+1}) become cc-tangent-connected and E_O becomes bounded. Now, we prove that if all pairs (p_i,p_{i+1}) are cc-tangent-connected, then $E_O\circ\eta$ decreases. Using equation (5) we compute

$$\begin{aligned}\dot{p}_i &= \gamma'(s_i)\dot{s}_i = \|\gamma'(s_i)\|\mathbf{t}_i\dot{s}_i = \mathbf{t}_i\,\text{sat}_v((d_i^+)^2-(d_i^-)^2)\\ \implies\quad \dot{s}_i &= \frac{\text{sat}_v((d_i^+)^2-(d_i^-)^2)}{\|\gamma'(s_i)\|},\end{aligned}$$

and therefore:

$$\begin{aligned}\frac{dE_O(p_1,\dots,p_N)}{dt} &= \sum_{i=1}^N \frac{\partial E_O(p_1,\dots,p_N)}{\partial\alpha_i}\frac{\partial\alpha_i}{\partial\mathbf{t}_i}\cdot\frac{\partial\mathbf{t}_i}{\partial s_i}\dot{s}_i\\ &= \sum_{i=1}^N \kappa(s_i)\,\frac{((d_i^-)^2-(d_i^+)^2)\,\text{sat}_v((d_i^+)^2-(d_i^-)^2)}{2\|\gamma'(s_i)\|}.\end{aligned}$$

Because we assumed $\kappa>0$ on the entire boundary, the cost function E_O decreases monotonically along the trajectories of equation (5). Using the LaSalle Invariance Principle, it can be proved that the p_i's will asymptotically converge to the set of critical configurations for E_O.

Let $\mathbf{s}(t) = [s_1(t),\dots,s_N(t)]^T\in\mathbb{T}^N$, and note that if ∂Q is analytic then E_O is analytic. Next, we recall a result from [1]. If there exists $\delta>0$ and τ such that, for all $t>\tau$, the following holds

$$\frac{dE_O}{dt} \equiv \langle\nabla E_O(\mathbf{s}(t)),\dot{\mathbf{s}}(t)\rangle \le -\delta\|\nabla E_O(\mathbf{s}(t))\|\|\dot{\mathbf{s}}(t)\|,$$

then $\mathbf{s}(t)$ converges to a unique critical configuration $\mathbf{s}^*$. We use this result as follows. Note that as $t\to+\infty$, $\mathbf{s}(t)$ approaches the set of critical configurations. We can then conclude that there exists a time τ after which sat_v is not active any longer and, hence, $\dot{s}_i(t) = -\lambda_i(t)\frac{\partial E_O}{\partial s_i}$, where $\lambda_i(t) = \frac{2}{\kappa(s_i)\|\gamma'(s_i)\|}$. Therefore we have

$$\begin{aligned}\langle\nabla E_O(\mathbf{s}(t)),\dot{\mathbf{s}}(t)\rangle &= -\nabla E_O(\mathbf{s}(t))^T\Lambda(t)\nabla E_O(\mathbf{s}(t))\\ &\le -\lambda_{\min}(t)\|\nabla E_O(\mathbf{s}(t))\|^2\,,\end{aligned}$$

where $\Lambda(t)\in\mathbb{R}^{N\times N}$ is a diagonal matrix with entries $[\Lambda(t)]_{ii} = \lambda_i(t)>0$, and $\lambda_{\min}(t) = \min\{\lambda_1(t),\dots,\lambda_N(t)\}$. We require:

$$-\lambda_{\min}(t)\|\nabla E_O(\mathbf{s}(t))\|^2 \le -\delta\|\nabla E_O(\mathbf{s}(t))\|\|\dot{\mathbf{s}}(t)\|\,,$$

or equivalently

$$\lambda_{\min}(t)\|\nabla E_O(\mathbf{s}(t))\| \ge \delta\|\dot{\mathbf{s}}(t)\|\,.$$

Note that $\|\dot{\mathbf{s}}(t)\| \le \lambda_{\max}(t))\|\nabla E_O(\mathbf{s}(t))\|$, where $\lambda_{\max}(t) = \max\{\lambda_1(t),\dots,\lambda_N(t)\}$, therefore:

$$\delta = \inf_{t>\tau}\frac{\lambda_{\min}(t))\|\nabla E_O(\mathbf{s}(t))\|}{\|\dot{\mathbf{s}}(t)\|} \ge \inf_{t>\tau}\frac{\lambda_{\min}(t)}{\lambda_{\max}(t)} > 0.$$

We can then conclude that the p_i's will asymptotically converge to a unique critical configuration for E_O.

Remark 4.3 (Implementation by group of robots) To dynamically construct the best outer-polygon approximation according to equation (5), the robots need to exchange information not only about their positions (like for the inner-polygon approximation) but also about their local tangent. •

4.1 Discrete-time outer-polygon approximation algorithms

It is easy to prove that an algorithm analogous to Algorithm 1 in the previous section guarantees convergence to the critical configuration of E_O. We state the analogous results here omitting the corresponding proof.

Given a strictly convex set Q, define $q_{\min}\colon (\partial Q)^2 \to \partial Q$ as follows: $q_{\min}(q_1, q_2)$ is the point of the counterclockwise arc from q_1 to q_2 whose tangent to ∂Q satisfies $d_i^- = d_i^+$. Note that $q_{\min}(q_1, q_2)$ minimizes $q \mapsto \mathrm{Area}(P_O(q_1, q, q_2))$.

Algorithm 3. At each discrete time instant $k \in \mathbb{N}$ and for each node $i \in \{1, \dots, N\}$ define:

$$p_i(k+1) = \begin{cases} q_{\min}(p_{i-1}(k), p_{i+1}(k)), & \text{if } i \equiv k \mod N, \\ p_i(k), & \text{if } i \not\equiv k \mod N\,. \end{cases} \tag{6}$$

Proposition 4.4 (Convergence of Algorithm 3) *If $k \mapsto \eta(k) = (p_1(k), \dots, p_N(k))$ denotes a trajectory of the dynamical system (6), then $E_O \circ \eta$ is monotonic non-increasing and η converges asymptotically to the set of critical configurations of E_O.*

Remark 4.5 Similarly to Algorithm 2 in the inner-polygon approximation problem, it is possible to design a discrete time algorithm based on admissible quintuplets. Such algorithm would have limitations similar to the ones of Algorithm 2 and we do not present it here in the interest of brevity.

5 "Outer minus inner" polygon approximation algorithms

An alternative cost function that quantifies the accuracy of a polygonal approximation of a convex body Q, is provided by the symmetric difference error E_S. In this section we provide a novel expression for $\frac{\partial E_S}{\partial p_i}$, $i \in \{1, \dots, N\}$ under the assumption that the outer polygon is bounded. This expression leads to a new type of gradient decent algorithm.

Lemma 5.1 (Partial derivative of E_S) *If (p_i, p_{i+1}) is cc-tangent-connected, then the area of the triangle formed by the segment $\overline{p_{i+1}p_i}$ and the rays $\ell^+(p_i)$ and $\ell^-(p_{i+1})$ is*

$$A_i(p_i, p_{i+1}, \mathbf{n}_i, \mathbf{n}_{i+1}) = \frac{1}{2} \frac{(\mathbf{n}_i \cdot (p_i - p_{i+1}))(\mathbf{n}_{i+1} \cdot (p_i - p_{i+1}))}{(\mathbf{n}_i \times \mathbf{n}_{i+1}) \cdot \mathbf{e}_3}.$$

Regarding p_i and $\mathbf{n}_i = \mathbf{n}(p_i)$ as a functions of the parameter $s_i \in [0, 1]$, we have

$$\frac{\partial E_S(p_1, \dots, p_N)}{\partial s_i} = \left(\frac{\partial A_{i-1}}{\partial p_i} + \frac{\partial A_i}{\partial p_i} - \kappa(s_i) \left(\frac{\partial A_{i-1}}{\partial \mathbf{n}_i} + \frac{\partial A_i}{\partial \mathbf{n}_i} \right) \right) \cdot \mathbf{t}_i.$$

PROOF. In the interest of space, we only mention here that the proof is based upon elementary calculations.

If we set $p_i = (x_i, y_i)$, $\mathbf{n}_i = (n_i^1, n_i^2)$ and $\mathbf{n}_{i-1} \times \mathbf{n}_i^+ := n_{i-1}^1 n_i^2 + n_i^1 n_{i-1}^2$, then explicit expressions for the relevant partial derivatives in Lemma 5.1 are:

$$\begin{aligned} \frac{\partial A_{i-1}}{\partial x_i} &= \frac{(p_i - p_{i-1}) \cdot (\, 2 n_{i-1}^1 n_i^1,\, \mathbf{n}_{i-1} \times \mathbf{n}_i^+ \,)}{2(\mathbf{n}_{i-1} \times \mathbf{n}_i^+)}\,, \\ \frac{\partial A_{i-1}}{\partial y_i} &= \frac{(p_i - p_{i-1}) \cdot (\, \mathbf{n}_{i-1} \times \mathbf{n}_i^+,\, 2 n_{i-1}^1 n_i^1 \,)}{2(\mathbf{n}_{i-1} \times \mathbf{n}_i^+)}\,, \\ \frac{\partial A_{i-1}}{\partial n_i^1} &= \frac{n_i^2 (\mathbf{n}_{i-1} \cdot (p_i - p_{i-1})^2)}{2(\mathbf{n}_{i-1} \times \mathbf{n}_i^+)^2}\,, \\ \frac{\partial A_{i-1}}{\partial n_i^2} &= \frac{n_i^1 (\mathbf{n}_{i-1} \cdot (p_i - p_{i-1})^2)}{2(\mathbf{n}_{i-1} \times \mathbf{n}_i^+)}. \end{aligned}$$

Lemma 5.2 (Gradient flow for E_S) *If $t \mapsto \eta(t) = (p_1(t), \dots, p_N(t))$ denotes a trajectory of the dynamical system*

$$\dot{p}_i = -\,\mathbf{t}_i \left(\frac{\partial A_{i-1}}{\partial p_i} + \frac{\partial A_i}{\partial p_i} - \kappa(s_i) \left(\frac{\partial A_{i-1}}{\partial \mathbf{n}_i} + \frac{\partial A_i}{\partial \mathbf{n}_i} \right) \right) \cdot \mathbf{t}_i\,, \quad i \in \{1, \dots, N\},$$

with $E_S \circ \eta(0) < +\infty$, then $E_S \circ \eta$ is monotonic non-increasing and η converges asymptotically to the set of critical configurations of E_S. Furthermore, if the boundary ∂Q is analytic, then η converges asymptotically to a critical configuration.

We omit the proof of this lemma as it closely parallels that of Lemma 3.1.

Remark 5.3 (Implementation by group of robots) Even for this scenarios, the robots can move along the gradient of E_S relying upon information that is available to them through one-hop communication and through sensing of local tangent and curvature data. •

6 Simulations

Figure 4 shows the implementation results of the three continuous time descent algorithms described in Sections 3, 4,and 5. The eleven nodes are on the contour described by $\gamma(\theta) = (2.1 + \sin(2\pi\theta))(\cos(2\pi\theta), \sin(2\pi\theta))^T$, for $\theta \in [0, 1)$. Figure 5 shows the implementation results

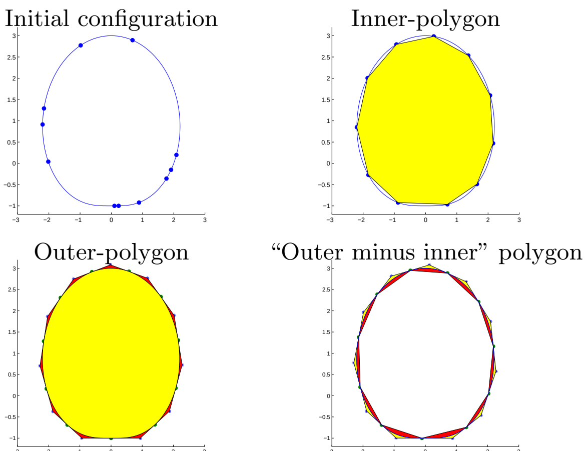

Fig. 4. From left to right and from top to bottom: initial condition of eleven nodes on a convex boundary, final condition after the implementation of the inner-polygon, outer-polygon, and "outer minus inner" polygon approximation algorithms.

of the discrete-time Algorithm 2 described in Sections 3.

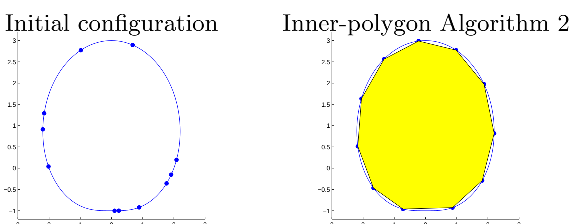

Fig. 5. From left to right: initial condition of eleven nodes on a convex boundary and final condition after the implementation of Algorithm 2.

7 Conclusions

We have discussed various geometric optimization problems and corresponding gradient flows. Future works will focus on nonsmooth contours such as polygons, nonconvex sets, and more general algorithms for optimal interpolation of boundaries.

Acknowledgements

This material is based upon work supported by NSF Award CMS-0442041 and ONR Award N00014-07-1-0721. An early version of this work appeared as [12].

References

[1] P.-A. Absil, R. Mahony, and B. Andrews. Convergence of the iterates of descent methods for analytic cost functions. *SIAM Journal on Control and Optimization*, 6(2):531–547, 2005.

[2] D. W. Casbeer, D. B. Kingston, R. W. Beard, T. W. Mclain, S.-M. Li, and R. Mehra. Cooperative forest fire surveillance using a team of small unmanned air vehicles. *International Journal of Systems Sciences*, 37(6):351–360, 2006.

[3] J. Clark and R. Fierro. Mobile robotic sensors for perimeter detection and tracking. *ISA Transactions*, 46(1):3–13, 2007.

[4] P. M. Gruber. Approximation of convex bodies. In P. M. Gruber and J. M. Willis, editors, *Convexity and its Applications*, pages 131–162. Birkhäuser Verlag, 1983.

[5] U. Helmke and J. B. Moore. *Optimization and Dynamical Systems*. Springer Verlag, New York, 1994.

[6] H. H. Johnson and A. Vogt. A geometric method for approximating convex arcs. *SIAM Journal on Applied Mathematics*, 38(2):317–325, 1980.

[7] M. Kass, A. Witkin, and D. Terzopoulos. Snakes: Active contour models. *International Journal of Computer Vision*, 1(4):321–331, 1987.

[8] J. P. LaSalle. *The Stability and Control of Discrete Processes*, volume 62 of *Applied Mathematical Sciences*. Springer Verlag, New York, 1986.

[9] S. Łojasiewicz. Sur les trajectoires du gradient d'une fonction analytique. *Seminari di Geometria 1982-1983*, pages 115–117, 1984. Istituto di Geometria, Dipartimento di Matematica, Università di Bologna, Bologna, Italy.

[10] D. Marthaler and A. L. Bertozzi. Tracking environmental level sets with autonomous vehicles. In *Conference on Cooperative Control and Optimization*, Gainesville, FL, December 2002.

[11] L. Scardovi, A. Sarlette, and R. Sepulchre. Synchronization and balancing on the *N*-torus. *Systems & Control Letters*, 56(5):335–341, 2007.

[12] S. Susca, S. Martínez, and F. Bullo. Distributed algorithms for polygonal approximation of convex contours. In *IEEE Conf. on Decision and Control*, pages 6512–6517, San Diego, CA, December 2006.

[13] E. Trost. Über eine Extremalaufgabe. *Nieuw Archief voor Wiskunde*, 2:1–3, 1949.

[14] F. Zhang and N. E. Leonard. Generating contour plots using multiple sensor platforms. In *IEEE Swarm Intelligence Symposium*, pages 309–316, Pasadena, CA, June 2005.